Local order and magnetism in liquid Al-Pd-Mn alloys

V. Simonet and F. Hippert
Laboratoire de Physique des Solides (UA CNRS 02), Université Paris–Sud, 91405 Orsay Cedex, France

H. Klein and M. Audier
LTPCM (UMR CNRS 5614), ENSEEG, Boîte Postal 75, 38402 Saint Martin d'Hères, France

R. Bellissent
Laboratoire Léon Brillouin (CEA-CNRS), CE Saclay, 91191 Gif sur Yvette Cedex, France

H. Fischer and A. P. Murani
Institut Laue-Langevin, Boîte Postal 156, 38042 Grenoble Cedex, France

D. Boursier
LMGP (UA CNRS 1109), INPG, Boîte Postal 45, 38402 Saint Martin d'Hères, France
(Received 20 January 1998; revised manuscript received 14 May 1998)

We report neutron scattering experiments on several Al-Pd-Mn liquid alloys with Mn content between 3.5 and 7.2 at. % which are in thermodynamical equilibrium with icosahedral quasicrystalline or approximant phases. The results reveal an overall similarity between the structure factor in the solid and in the liquid states, suggesting the presence of a strong icosahedral local order in the liquid state. Simulations of the structure factor at large momentum transfer support this interpretation. In addition, a marked increase of the neutron scattering cross section at small momentum transfer occurs on melting, revealing the appearance of paramagnetic scattering in the liquid state. A comparison with susceptibility measurements combined with additional neutron scattering experiments using polarized neutrons, demonstrates that magnetic moments are present in the liquid state and not in the solid state. In the liquid state, at a given temperature, the same spin value can be extracted from the paramagnetic scattering and the susceptibility data. The link between the evolution of the magnetic properties and that of the short- and medium-range order at the melting point is discussed. Surprisingly, the paramagnetism continues to increase with temperature in the liquid state. This remarkable behavior might be due either to an increase of the spin value with temperature as a consequence of thermal expansion or to the coexistence of magnetic and nonmagnetic Mn in temperature-dependent proportions. The origin of this behavior is discussed in relation to the evolution of the liquid structure. [S0163-1829(98)07033-7]

I. INTRODUCTION

The discovery of quasiperiodic structures with icosahedral symmetry by Shechtman *et al.* in 1984 (Ref. 1) has aroused interest in the study of the relationship between short-range icosahedral order in liquid alloys or metallic glasses and the long-range order in this new state of matter.[2,3] Previously, the idea that structures of liquid metals could be based on packings of icosahedral units was suggested by Frank in order to explain supercooling effects.[4] Even though this property was later confirmed by molecular dynamics simulations of supercooled liquids,[5] experimental proof is still required. Let us recall that the first quasicrystalline samples of Shechtman *et al.* (Ref. 1) were obtained by melt spinning of liquid Al-Mn and Al-Cr alloys. Since these compounds were metastable, several authors[6] first attempted to describe their structure by icosahedral glass models which display long-range orientational order, but only short-range translational order, which would lead to rather sharp diffraction peaks in accordance with experimental diffraction patterns observed on these first materials. Alternatively, the possibility of an icosahedratic phase (i.e., a three-dimensional generalization of the two-dimensional hexatic phase) has also been discussed.[7] However, these models were progressively abandoned when stable quasicrystalline phases exhibiting Bragg peaks as narrow as those of periodic crystals of good quality were found in, for instance, Al-Fe-Cu and Al-Pd-Mn phases. From several diffraction studies, it was shown that both orientational order and long-range quasiperiodic translational order occur in these stable phases[8,9] which exhibit anomalous transport properties such as a very high resistivity.[10] Most structural models involve packings of various icosahedral clusters with a large number of atoms, such as Mackay clusters (54 atoms) in Al-Pd-Mn quasicrystals or Bergman clusters (104 atoms) in Al-Li-Cu quasicrystals.[11] The same clusters are also found in the approximants of quasicrystals, which are periodic phases with large unit cells whose structures are closely related to that of quasicrystals.[12] Clusters are not only a convenient geometrical description of these complex phases but indeed play a role in their properties.[13,14] Therefore, in the case of liquid-icosahedral solid phase equilibrium, it might be expected that the local order in liquids forming quasicrystals reflects the local organization of atoms in the solid. Although the results of previous studies on liquid $Al_{80}Mn_{20}$ and $Al_{71}Pd_{19}Mn_{10}$ alloys[15,16] suggest the presence of local icosahedral order in these liquid states, no di-

rect comparison has yet been made with the local order in the solid state.

On the basis of results of a previous study of the Al-Pd-Mn phase diagram in the region of quasicrystalline phases,[17,18] we considered it interesting to compare carefully the local order in liquid phases and in quasicrystalline or approximant equilibrium phases for several compositions. Al-Pd-Mn alloys (with Mn content between 3.5 and 7.2 %) are interesting for such a study for the following reasons. (i) The structures of several complex approximant Al-Pd-Mn phases have been recently solved and their decorations in terms of icosahedral clusters have been well established.[19] (ii) The structural models of the quasicrystalline phase are very detailed and here again their decoration, although not completely solved, implies the packing of icosahedral units (Ref. 9). (iii) The melting is nearly congruent and thus the icosahedral or approximant phases obtained by primary crystallization have a composition close to that of the liquid. Additional interest in studying liquid Al-Pd-Mn alloys was raised by our first neutron scattering results[20] that suggested the appearance of localized moments in the liquid state. Thus a possible correlation between the variations of the icosahedral order and of the magnetic properties with temperature could be considered. Moment formation in icosahedral and approximant phases[21,22] is affected by the presence of a pseudogap in the density of states at the Fermi level.[23] Hence, it is to be expected that melting strongly affects the electronic properties, and thereby magnetism as well. Therefore the aims of the present investigation are first to carry out an extensive study of the magnetic properties of liquid Al-Pd-Mn alloys in order to determine their composition and temperature dependences, secondly to determine local order in the liquid alloy through comparison with local order in the solid, and finally to examine the interplay between magnetic properties and local order (short and medium range) in the solid and in the liquid.

In the present paper, after a brief description of the Al-Pd-Mn samples (Sec. II), we present the main features deduced from neutron scattering experiments (Sec. III). Section IV is devoted to magnetic properties. The occurrence of paramagnetic neutron scattering in the liquid state is first established (Sec. IV A). This magnetism is thoroughly studied by susceptibility and polarized neutron scattering measurements (Secs. IV B and IV C) which in addition show that the solids are nonmagnetic. Then by carefully comparing neutron and susceptibility data (Sec. V A) we establish the presence of localized magnetic moments on Mn atoms in the liquid state and estimate their spin value. In Sec. V B, we try to characterize the local order in the solid and liquid states in the framework of the Sachdev and Nelson theory (Refs. 2,3) and by simulations of the structure factors at large momentum transfer Q ($Q \geqslant 4.5$ Å^{-1}). Finally in Sec. VI, we discuss the possible origin of the magnetic moments in the liquid state, and of the striking temperature dependence of the magnetic properties, in connection with the temperature evolution of short- and medium-range structural order at the melting point and in the liquid state.

II. SAMPLES

We prepared five Al-Pd-Mn alloys with the following compositions: $Al_{72.1}Pd_{20.7}Mn_{7.2}$ $Al_{77}Pd_{18}Mn_5$, $Al_{79.8}Pd_{16.6}Mn_{3.6}$, $Al_{76.5}Pd_{20}Mn_{3.5}$ and $Al_{79.1}Pd_{19.2}Mn_{1.7}$, and one binary alloy $Al_{81}Pd_{19}$. High purity constituent elements (Al 99.999 wt. %, Pd and Mn 99.9 wt. %) were melted in a cold crucible induction furnace under argon atmosphere. The compositions were chosen according to the results of a metallurgical investigation related to thermodynamic liquid-solid equilibria of the Al-Pd-Mn phase diagram in the region of the quasicrystalline phase field (Ref. 17). In particular, composition ranges of liquidus phase fields in equilibrium with icosahedral and approximant phases were determined from this study. As each of these solid phases exhibits a noncongruent melting, their composition lies outside of the composition range of their corresponding liquidus phase field.

Thus, the compositions of samples $Al_{72.1}Pd_{20.7}Mn_{7.2}$ (a) and $Al_{77}Pd_{18}Mn_5$ (b) were chosen such that a primary crystallization of quasicrystalline icosahedral phase [whose composition lies in the range of Al(68 to 69.5), Pd(20.3 to 23.2), Mn(8 to 10.2)] was obtained through a normal alloy casting. Subsequent crystallizations of other phases in these samples were determined by standard methods: differential thermal analyses, chemical composition analyses by x-ray wavelength spectroscopy and structure analyses either by x-ray or electron diffraction. These phases are approximants of the icosahedral structure, called ξ' [in the range Al(73 to 74), Pd(21.6 to 23), Mn(4 to 4.4)] and R (Al 78.6, Pd 5.7, Mn 15.6), and an Al-rich ternary eutectic (Al/ξ'/R) (Ref. 17). The proportion of icosahedral phase present in sample (a) is large (about 60 vol. %). It is much less in the sample (b) (about 10 vol. %), for which the majority phase is the ξ' approximant (about 60 vol. %). For the three other ternary sample compositions that we have studied, $Al_{79.8}Pd_{16.6}Mn_{3.6}$ (c), $Al_{76.5}Pd_{20}Mn_{3.5}$ (d) and $Al_{79.1}Pd_{19.2}Mn_{1.7}$ (e), the primary crystallization under normal casting conditions corresponds to the formation of the ξ' approximant phase, whose proportion varies as a function of the initial liquid alloy composition. The binary alloy $Al_{81}Pd_{19}$ (f) consists mainly of an orthorhombic Al_3Pd phase,[24] nearly isomorphous with the ξ' approximant, and a eutectic Al/Al_3Pd phase. As determined from differential thermal analysis, the transformation temperatures corresponding to the beginning of primary crystallization from the liquid phase (T_L) are 1160, 1122, 1096, 1118, 1125, and 1050 K for the different samples (a)–(f) respectively. For each ternary sample, the solidification ends with the formation of the ternary eutectic at an invariant temperature of $T_E = 890 \pm 5$ K. The melting point of the binary eutectic Al/Al_3Pd is 888 K.

III. STRUCTURE FACTORS

A. Experimental

Neutron scattering experiments were performed on the spectrometer 7C2 of the Orphée reactor, at LLB (CE Saclay), on $Al_{72.1}Pd_{20.7}Mn_{7.2}$, $Al_{77}Pd_{18}Mn_5$, and $Al_{76.5}Pd_{20}Mn_{3.5}$ samples, in the solid and liquid states up to 1300 K. The scattered intensities were measured using a fixed 640-cell detector in a momentum transfer (Q) range of 0.5 (or 0.7) -16 Å^{-1} and with an incident neutron wavelength λ of 0.7046 Å. The samples were heated in a vanadium resistor furnace. Further experiments were carried out on the spectrometer D4B of the high flux reactor at ILL (Grenoble), on

an $Al_{72.1}Pd_{20.7}Mn_{7.2}$ sample up to 1923 K, using λ of 0.7026 Å. The scattered intensities were measured through two 64-cell moving detectors in a Q range of 0.2–14 $Å^{-1}$. The high temperatures were reached by using a tungsten resistor furnace[25] and measured with a two-color optical pyrometer. The samples were melted in single crystal sapphire containers which do not react with molten Al-Pd-Mn alloys. The orientation of each container around the vertical axis (perpendicular to the scattering plane) was set such that no Bragg reflection could be detected. However, because of the low resolution in Q space of the two spectrometers, Bragg contaminations could not be completely eliminated. The scattering of the empty container was then measured at temperatures corresponding to those of the experiment before introducing the sample. The sample masses (cylindrical ingots) were between 13 and 17 g.

At a given temperature the differential scattering cross section of the sample $(d\sigma/d\Omega)(Q)$ was obtained by subtracting from the spectrum of the full container, the spectrum of the empty sapphire container within the furnace, multiplied by a temperature-independent proportionality coefficient α, and the spectrum of the empty furnace, multiplied by $1-\alpha$. For each sample the α value was adjusted so that any trace of the sapphire scattering could not be detected in the final spectra. The α values were found to vary between 0.91 and 0.93 for the different samples. They are in agreement with the transmission factor calculated following the method of Paalman and Pings[27] provided that both the scattering and absorption processes are taken into account. Plazeck corrections for inelastic scattering[28,29] and a standard multiple scattering correction[30] were carried out. A vanadium sample with a geometry identical to that of the Al-Pd-Mn samples was measured in order to get an absolute normalization of the cross sections. In all cases the asymptotic value of $4\pi(d\sigma/d\Omega)(Q)$ at large Q coincides, within a few percent, with the calculated total scattering cross section $\sigma_T=\sigma_i+4\pi\langle b^2\rangle$, where $\sigma_i=\Sigma c_j\sigma_{\rm inc}^j$ and $\langle b^2\rangle=\Sigma c_j\overline{b_j}^2$. [$\sigma_{\rm inc}^j$ is the intrinsic incoherent scattering cross section (isotopic and nuclear spin mixture contributions), $\overline{b_j}$ the average scattering length, and c_j the concentration of the jth element (Al, Pd, or Mn) (Ref. 26).] Such agreement validated the corrections applied to the measured neutron intensities. In the following we have normalized the data so that the asymptotic value of the differential scattering cross section at large Q is equal to σ_T. The experimental structure factor $S_{\rm exp}(Q)$ is related to the differential scattering cross section by $S_{\rm exp}(Q)=[4\pi(d\sigma/d\Omega)(Q)-\sigma_i]/4\pi\langle b^2\rangle$, i.e., normalized to unity.

B. Results

Neutron scattering spectra measured on the $Al_{72.1}Pd_{20.7}Mn_{7.2}$ alloy at 1103 K where the eutectic was molten (and hence the solid icosahedral phase coexisted with a small fraction of liquid) and at 1223 K just above the melting point ($T_L=1160$ K) are shown in Fig. 1(a). The broad maxima of the differential scattering cross section in the liquid state correspond to the main Bragg peak groups of the icosahedral phase. The similarity between the liquid and solid spectra extends up to the largest Q values as can be seen in Fig. 2. The neutron scattering spectra measured on the $Al_{76.5}Pd_{20}Mn_{3.5}$ alloy at 873 K, where the sample was entirely solid consisting mainly of the ξ' approximant phase, and at 1223 K in the liquid state ($T_L=1118$ K) are shown in Fig. 1(b). Although the Bragg peaks in Fig. 1(b) differ slightly from those of the icosahedral phase in Fig. 1(a), an overall similarity between both sets of spectra is observed. The same kind of observation holds for the $Al_{77}Pd_{18}Mn_5$ alloy. Figure 3 shows that the experimental structure factors of these three alloys at 1223 K (i.e., just above their liquidus temperature) are indeed extremely similar, except at small Q values where paramagnetic scattering contributions are superimposed on the measured structure factor, as will be explained in Sec. IV A. Such observations suggest the presence of strong local order in the liquid state above T_L, reminiscent of that in the solid.

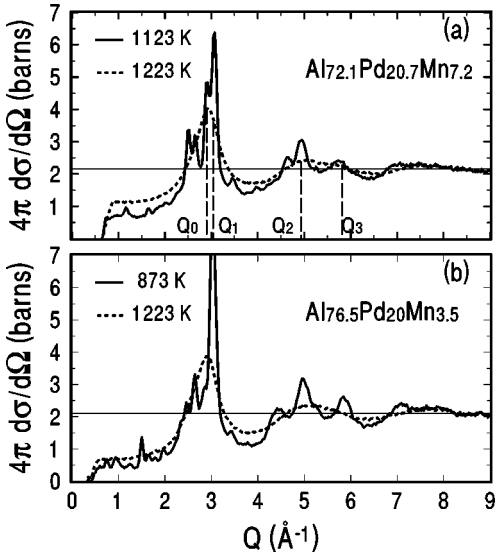

FIG. 1. Comparison of the neutron differential scattering cross section $(4\pi d\sigma/d\Omega)$ in barns versus Q in the solid and in the liquid states. (a) $Al_{72.1}Pd_{20.7}Mn_{7.2}$: the Bragg peaks characteristic of icosahedral order, according to Ref. 3, are indicated by vertical lines ($Q_0=2.905$ $Å^{-1}$, $Q_1=1.052Q_0$, $Q_2=1.701Q_0$, and $Q_3=2.00Q_0$) and the horizontal line indicates the total scattering cross section $\sigma_T=2.166$ b. (b) $Al_{76.5}Pd_{20}Mn_{3.5}$: the horizontal line indicates $\sigma_T=2.122$ b.

We have therefore searched for a possible evolution of the neutron scattered intensity with increasing temperature in the

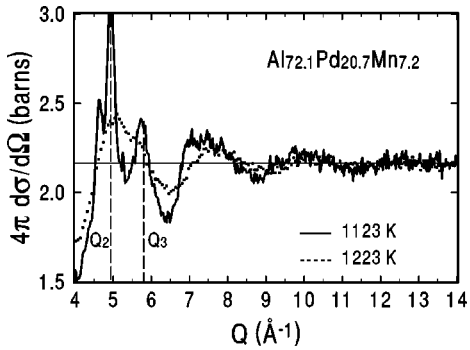

FIG. 2. Neutron differential scattering cross section at large Q in the liquid (1223 K) and in the solid icosahedral phase (1123 K) in $Al_{72.1}Pd_{20.7}Mn_{7.2}$. [The data at smaller Q are shown in Fig. 1(a)]. Q_2 and Q_3 have the same meaning as in Fig. 1(a).

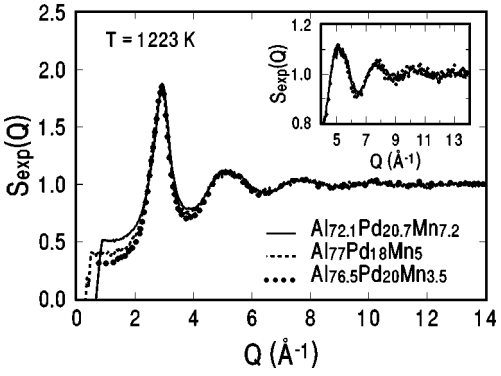

FIG. 3. Comparison of the experimental liquid structure factors $S_{exp}(Q)$ at 1223 K for three Al-Pd-Mn alloys. The three curves are almost indiscernible for $Q \geq 5$ Å^{-1} (inset).

liquid state. This study was performed up to 1923 K, using the spectrometer D4B, on the $Al_{72.1}Pd_{20.7}Mn_{7.2}$ alloy whose primary crystallization gives rise to the largest proportion of icosahedral phase. Results are shown in Fig. 4. As expected in liquid metallic alloys, the oscillations of the structure factor are broadened and their amplitudes decrease with increasing temperature. An evolution of the liquid structure is suggested by the fact that the shoulder on the second peak (around 5.5 Å^{-1}), well defined just above the melting point, is progressively damped with increasing temperature. Finally it must be emphasized that the oscillations at larger Q remain well defined up to 1923 K.

IV. MAGNETISM

A. Paramagnetic neutron scattering

Another peculiar feature we noticed for all the alloys in the neutron scattering experiments is that a marked increase of the differential scattering cross section at small Q occurs when the temperature increases from T_E to T_L (Fig. 1). In the liquid, above T_L, it continues to increase with temperature but with a much smaller slope. We shall show that part of these effects results from variations of the paramagnetic scattering. In Fig. 5, the differential scattering cross section $4\pi(d\sigma/d\Omega)(Q)$ at 0.2 Å^{-1} (σ_0) measured on the

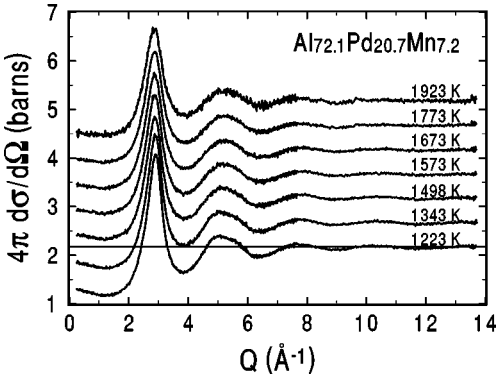

FIG. 4. Temperature evolution of the neutron differential scattering cross section for $Al_{72.1}Pd_{20.7}Mn_{7.2}$ in the liquid state, measured with the D4B spectrometer. The vertical scale (in b) corresponds to the data measured at 1223 K. The curves at successive temperatures have been shifted by steps of 0.5 b.

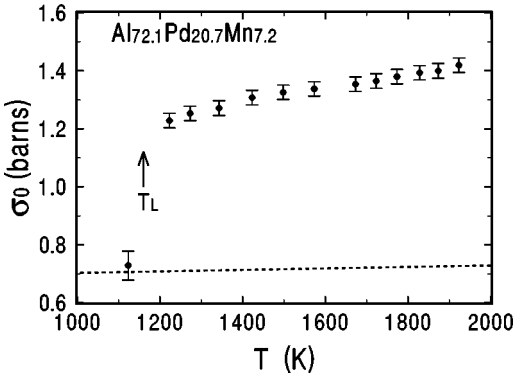

FIG. 5. Temperature dependence of the differential scattering cross section ($\sigma_0 = 4\pi d\sigma/d\Omega$) at $Q = 0.2$ Å^{-1} in $Al_{72.1}Pd_{20.7}Mn_{7.2}$. The dashed line indicates the maximum value of σ_0 in the absence of paramagnetic scattering (see text). At the lowest temperature (1123 K) the sample is a mixture of liquid and solid icosahedral phase.

$Al_{72.1}Pd_{20.7}Mn_{7.2}$ alloy is plotted as a function of temperature from 1123 K up to 1923 K. In the liquid state, σ_0 is obtained by calculating the mean value of $4\pi(d\sigma/d\Omega)(Q)$ in a small Q range around 0.2 Å^{-1} and the error bar is equal to the statistical error. In the solid state, the presence of Bragg peaks leads to overestimated σ_0 values. This is the reason why the error bars for the solid state are larger than those for the liquid state. Note that another type of error comes from uncertainties in the various corrections applied to the measured neutron spectra (Sec. III A). They lead to an overall shift of the σ_0 data in Fig. 5 but do not affect relative variations with temperature. Such errors, estimated to be of the order of ± 0.06 b, are not included in the statistical error bars shown in Fig. 5.

The differential scattering cross section at small Q is a sum of different contributions that we have to evaluate in order to deduce that of the paramagnetic scattering. Several physical processes must be considered: the density fluctuation term σ_d, the intrinsic incoherent scattering (isotopic and nuclear spin) σ_i, the chemical incoherent scattering resulting from the mixture of the different elements σ_c whose maximum value is given by $4\pi(\langle b^2\rangle - \langle b\rangle^2)$, and the paramagnetic scattering $4\pi(d\sigma_p/d\Omega)(Q)$; thus,

$$4\pi\frac{d\sigma}{d\Omega}(Q) = \sigma_d + \sigma_i + \sigma_c + 4\pi\frac{d\sigma_p}{d\Omega}(Q). \qquad (4.1)$$

The density fluctuation term σ_d is equal to $k_B T \rho_0 \kappa_T 4\pi\langle b^2\rangle$ at $Q \to 0$, where ρ_0 is the number of atoms per unit volume and κ_T is the isothermal compressibility equal to $C_p/(C_v \rho v_s^2)$, where C_p (respectively, C_v) is the constant pressure (respectively, volume) heat capacity, ρ the mass density, and v_s the sound velocity of the alloy.[31] In most metallic liquid alloys, σ_d at $Q \to 0$ is about 2% of the $4\pi\langle b^2\rangle$ value.[32]

In the case of the $Al_{72.1}Pd_{20.7}Mn_{7.2}$ alloy, the nuclear incoherent scattering σ_i is equal to 0.054 b (Ref. 26) and σ_d can be accurately evaluated since the sound velocity in a similar alloy ($Al_{90}Mn_{10}$) was measured to be $v_s = 4400$ m s^{-1} at 1223 K.[33] The corresponding value of $k_B T \rho_0 \kappa_T$ is equal to 0.014, using a ratio value of C_p/C_v

$=1.15$,[34] and then σ_d is equal to 0.03 b. Then, from the measured σ_0 value, we can deduce the sum of the chemical incoherent scattering and of the paramagnetic scattering at $Q=0.2$ Å^{-1}. Further analysis involves a separation of these two contributions. However, we can already notice that the measured σ_0 value at 1223 K (1.2 ± 0.06 b) is larger than 0.71 b obtained by summing σ_d, σ_i, and the maximum chemical incoherent scattering ($\sigma_c=0.624$ b). This proves the existence of paramagnetic scattering whose minimal value is therefore 0.49 b. The increase of σ_0 during melting can result from an increase of either the chemical incoherent scattering only the paramagnetic scattering only, or both. In order to separate these two effects we performed two other kinds of experiments: magnetic susceptibility measurements as a function of temperature (Sec. IV B) and polarized neutron scattering (Sec. IV C).

B. Magnetic susceptibility

Using a Faraday balance, variations of the susceptibility were measured as a function of temperature on six samples (a) $Al_{72.1}Pd_{20.7}Mn_{7.2}$, (b) $Al_{77}Pd_{18}Mn_5$, and (d) $Al_{76.5}Pd_{20}Mn_{3.5}$, previously studied by neutron scattering, and (c) $Al_{79.8}Pd_{16.6}Mn_{3.6}$, (e) $Al_{79.1}Pd_{19.2}Mn_{1.7}$, and (f) $Al_{81}Pd_{19}$. The magnetization was measured in a constant magnetic field ($H=10$ kG), in the temperature range [300–1300 K]. The samples (mass$\simeq$0.1 g) were ground into powder, put in a small sapphire container, and introduced in a quartz tube sealed under vacuum. The temperature dependence of the magnetic susceptibility in the different alloys, $\chi=M/H$, is shown in Fig. 6. The contributions of the sapphire and quartz containers were found to be temperature independent and were subtracted. The temperature was changed by steps of 25 K every 35 min. Identical $\chi(T)$ curves were obtained for heating and cooling cycles. This reversibility suggests that the samples are in thermodynamic equilibrium above T_E. In Fig. 6 the error bars for the measurements are smaller than the size of the symbols. However, systematic errors in the susceptibility corrections (subtraction of the quartz and sapphire susceptibility) can cause an overall shift of the data. In order to evaluate this error, we systematically performed magnetization measurements, using a superconducting quantum interference device (SQUID) magnetometer, on all the samples previously measured with the Faraday balance. For each sample, a very slight correction ($\leqslant 6\times10^{-6}$ emu/mole) was required in order to make the susceptibility at 300 K coincide with the value determined using the SQUID magnetometer.

At room temperature, all the samples were found to be diamagnetic. No appreciable Curie terms were detected down to 4 K from the SQUID measurements, which establishes an absence of localized magnetic moments in all the phases contained in the solid samples (i.e., quasicrystalline phase, ξ' approximant phase, and eutectic). In the solid state, up to T_E, the magnetic susceptibility exhibits a T^2 dependence $[\chi(T)-\chi(T=0)\propto T^2]$, as previously observed in several quasicrystalline phases and ascribed to the presence of a pseudogap at the Fermi level.[35,36] The amplitude of the T^2 term decreases progressively, from 17×10^{-12} emu/(mole.K^2) in sample (a) to 4.7×10^{-12} emu/(mole.K^2) in sample (d), when the proportion

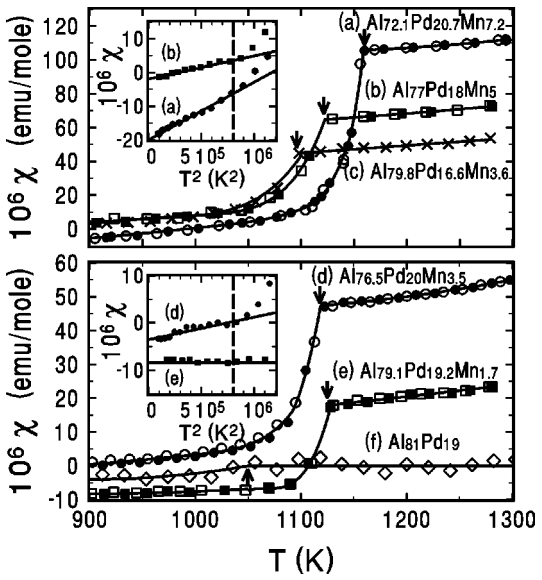

FIG. 6. Temperature dependence of the magnetic susceptibility during the solid-liquid transformation and in the liquid state, for the different Al-Pd-Mn alloys [samples (a)–(e)] and for the binary $Al_{81}Pd_{19}$ alloy [sample (f)]. For each alloy the liquidus temperature is indicated by an arrow. The statistical error bars are smaller than the size of the symbols. The solid lines are guides to the eye. Data measured when increasing (open symbols) and decreasing (close symbols) temperature are identical. [For sample (c) no distinction is made between data measured for increasing and decreasing temperature.] The susceptibility in the solid state is shown in the insets for samples (a), (b), (d), and (e). For samples (a), (b), and (d) a T^2 variation follows (solid line) up to the melting point of the ternary eutectic indicated by the vertical dashed line.

of icosahedral and approximant phases in the solid sample decreases. In sample (e), χ does not vary with T in the solid state, within the accuracy of the data. In all samples a clear change of regime occurs when the temperature reaches the melting temperature of the eutectic ($T_E=890$ K) as can be seen in the insets of Figs. 6(a) and 6(b). Above T_E, χ increases more rapidly with temperature than in the solid state. In the temperature range $[T_E-T_L]$ the slope $d\chi/dT$ increases continuously. At T_L an abrupt change of $d\chi/dT$ occurs. Above T_L in the liquid state, χ goes on increasing with temperature but with a much smaller slope. It is striking to note the similarity between the $\chi(T)$ (Fig. 6) and $\sigma_0(T)$ (Fig. 5) curves.

In the liquid state, at any fixed temperature, χ can be expressed as $A(T)+B(T)c$, where c is the Mn concentration of the alloy (Fig. 7): $A(T)\simeq0$ at all temperatures and $B(T)$ increases with temperature. There is perhaps a slight departure from this law for the more concentrated alloy $Al_{72.1}Pd_{20.7}Mn_{7.2}$. In spite of their different Al/Pd ratio, it is interesting to notice that the $Al_{76.5}Pd_{20}Mn_{3.5}$ and $Al_{79.8}Pd_{16.6}Mn_{3.6}$ alloys have almost the same susceptibility thus suggesting that Pd atoms do not influence the magnetic behavior. The observed linear concentration dependence of the susceptibility suggests a simple dilute alloy picture where magnetic atoms are diluted in a nonmagnetic matrix. To confirm this point, we studied the binary Al_{81} Pd_{19} alloy whose Al/Pd ratio is close to the Al/Pd ratios in the studied Al-Pd-Mn samples. Its magnetic susceptibility in the liquid state

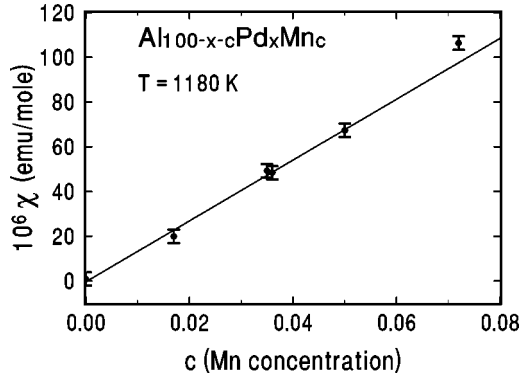

FIG. 7. Magnetic susceptibility at 1180 K versus the Mn concentration c in liquid Al-Pd-Mn alloys. The solid line is a linear fit of the data for $c \leqslant 0.05$: $\chi = A(T) + B(T)c$ with $A(T=1180\ \mathrm{K}) = (0 \pm 1) \times 10^{-6}$ emu/mole and $B(T=1180\ \mathrm{K}) = (1350 \pm 75) \times 10^{-6}$ emu/(mole Mn).

is temperature independent and nearly equal to zero [Fig. 6(b)] in agreement with the observation that the $A(T)$ term is close to zero at all temperatures.

In summary the susceptibility increase just above T_E in Al-Pd-Mn alloys is clearly due to the onset of melting. The continuous increase of χ between T_E and T_L reflects the increasing proportion of liquid in the solid-liquid mixture. A quantitative interpretation of this susceptibility variation is made difficult by the fact that liquid composition is changing continuously with temperature during the noncongruent melting (i.e., the Mn concentration in the liquid increases). The susceptibility in the liquid state appears to be proportional to the Mn content. This seems to exclude that the variation of χ on melting results from an increase of the Pauli susceptibility whose contribution to the paramagnetic neutron scattering would in any case be difficult to observe. This conclusion is further supported by the fact that only a very small susceptibility jump is observed in the binary $Al_{81}Pd_{19}$ alloy on melting. Therefore all these experimental results suggest that the magnetism in the liquid state is due to the formation of localized magnetic moments on Mn atoms.

C. Polarized neutron scattering

Polarized neutron scattering experiments were performed on the D7 spectrometer at ILL (Grenoble) with an incident neutron wavelength λ of 4.8 Å. The $Al_{72.1}Pd_{20.7}Mn_{7.2}$ alloy was studied at room temperature and at 1170 K, just above the liquidus temperature. Incident neutrons were sequentially polarized along the three perpendicular directions. For each direction of polarization, the spin-flip and non-spin-flip scatterings were alternatively measured. Paramagnetic and nuclear spin incoherent scatterings give rise to both spin-flip and non-spin-flip processes while the nuclear coherent and incoherent (isotopic and chemical) scatterings are non-spin-flip. By suitable combinations of the measured spin-flip and non-spin-flip signals, the contributions of the nuclear spin incoherent scattering, the nuclear scattering and the paramagnetic scattering can be determined.[37] A vanadium sample was measured to determine the detector efficiencies and to convert the measured intensities to barn. The contribution of the sample environment was subtracted. The measured spin-flip and non-spin-flip intensities were corrected taking into

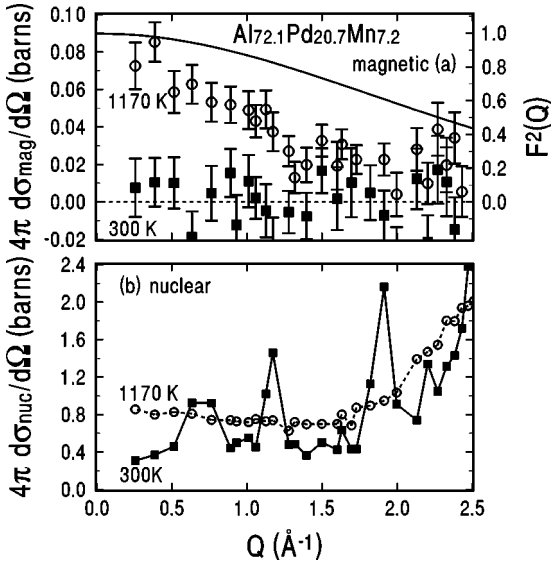

FIG. 8. Polarized neutron scattering measurements. (a): Q dependence of the differential paramagnetic scattering cross section in $Al_{72.1}Pd_{20.7}Mn_{7.2}$ at 300 K (full squares) and at 1170 K in the liquid state (open circles). There is paramagnetic scattering in the liquid state and no such signal in the solid state. The data in the liquid state, normalized to 1 at $Q=0$ (right vertical scale), are compared to the form factor of a free Mn^{2+} ion (solid line). (b): Differential nuclear scattering cross section at 300 and 1170 K [same symbols as in (a)].

account the finite value of the flipping ratio of the experimental setup (Ref. 37) determined from the scattering of a quartz glass sample (almost entirely non-spin-flip). A Monte Carlo program was used to compute the multiple scattering correction in a spin polarization analysis configuration taking into account the self-absorption correction for the Al-Pd-Mn and vanadium samples.

The differential magnetic scattering cross section at 300 and 1170 K (obtained by averaging spin-flip and non-spin-flip measurements) is shown in Fig. 8(a). Very large error bars are due to small counting rates resulting from the significant attenuation of the incident and scattered beams within the neutron polarizer and analyzer devices. Nevertheless, in agreement with previous results, paramagnetic scattering is detected in the liquid state while it is not measurable in the solid state. The differential nuclear scattering cross section is shown in Fig. 8(b) for the same temperatures. In the liquid, the first peak of the structure factor does not contribute to the measured signal for $Q \leqslant 1.6$ Å^{-1}. The nuclear signal decreases slightly from $Q=0.2$ up to 0.6 Å^{-1}. This relatively small effect could be due to the existence of density inhomogeneities leading to small angle scattering. It will be neglected in the following. For $0.6 \leqslant Q \leqslant 1.5$ Å^{-1} the nuclear signal is constant (equal to 0.7 ± 0.07 b). It is the sum of the density fluctuation term (0.03 b), the nuclear isotopic incoherent scattering whose maximum value is equal to 0.019 b,[38] and the chemical incoherent scattering. Therefore the chemical incoherent scattering contribution is equal to $\sigma_c = 0.65 \pm 0.07$ b. This value is in good agreement with the calculated maximal value of 0.624 b. In the solid, the nuclear incoherent scattering, measured between the Bragg peaks, reaches only 0.4 ± 0.1 b. Therefore we conclude that the

chemical incoherent scattering increases on melting and reaches its maximal value in the liquid state above T_L. Thus the increase of the differential scattering cross section measured with unpolarized neutrons on melting is not only due to the onset of paramagnetic scattering in the liquid but also to an increase of the chemical incoherent scattering.

Knowing the chemical incoherent scattering contribution, the differential paramagnetic scattering cross section in the liquid can be calculated from the differential scattering cross section measured using unpolarized neutrons [Eq. (4.1)]. In the $Al_{72.1}Pd_{20.7}Mn_{7.2}$ alloy, at 1223 K, from $\sigma_0 = 1.2 \pm 0.06$ b at $Q = 0.2$ Å^{-1}, one obtains $4\pi(d\sigma_p/d\Omega)(Q) = 0.49$ b which is much larger than the signal measured using polarized neutrons ($\simeq 0.075 \pm 0.015$ b). This discrepancy is probably due to the quasielastic nature of the paramagnetic scattering (see, for example, Ref. 39). On D7 the integration on energy is limited, on the neutron energy loss side, by the low incident neutron energy ($E_i = 3.5$ meV) and, on the neutron energy gain side, by an effective cutoff (around 10 meV) due to the progressive decrease of the efficiency of the neutron spin analyzers with increasing energy. On the contrary, the high incident energies used on the 7C2 and D4B spectrometers ($E_i \simeq 170$ meV) permit an integration of a much larger fraction, or almost the whole, of the paramagnetic response. Assuming the whole signal is integrated on 7C2 and D4B, then only 15% of the paramagnetic signal was detected on D7 at 1170 K.[40]

V. DATA ANALYSIS

A. Magnetism

In this section we compare the temperature dependence of the susceptibility and that of the paramagnetic scattering in the liquid state of the studied Al-Pd-Mn alloys, assuming the formation of localized moments in the liquid. We shall assume that all the Mn atoms bear the same spin S. In the quasistatic approximation, i.e., if the spectral extent of the paramagnetic scattering is less than $k_B T$, where T is the temperature of the measurement, and if the whole quasielastic paramagnetic scattering is integrated in energy, the differential paramagnetic scattering cross section can be expressed as[41]

$$4\pi \frac{d\sigma_p}{d\Omega}(Q) = 8\pi c r_0^2 \left(\frac{1}{2} g F(Q) \right)^2 \chi(Q) \frac{k_B T}{g^2 \mu_B^2}, \quad (5.1)$$

where $r_0 = -0.54 \times 10^{-12}$ cm, c is the Mn concentration, g is the Landé factor ($g = 2$ in the following), $\chi(Q)$ is the Q-dependent static susceptibility per Mn atom, $F(Q)$ is the magnetic form factor, i.e., the Fourier transform of the magnetization density on the Mn atom normalized to 1 when Q tends to 0, and the other symbols have their usual meaning. In the single ion limit, correlations between magnetic moments are negligible; the susceptibility is then Q independent, and $\chi(Q) = \chi(Q=0) = \chi/(cN_a)$, where χ is the bulk susceptibility per mole given by

$$\chi = c g^2 \mu_B^2 N_a \frac{S(S+1)}{3 k_B T} = C/T, \quad (5.2)$$

where C is the Curie constant. Hence the differential paramagnetic scattering cross section can be written as

$$4\pi \frac{d\sigma_p}{d\Omega}(Q) = \frac{8\pi}{3} c r_0^2 F(Q)^2 S(S+1), \quad (5.3)$$

and its Q dependence reproduces that of the squared magnetic form factor. It is quite evident that the susceptibility of the liquid Al-Pd-Mn alloys cannot be described by a simple Curie law, nor even a Curie-Weiss-like behavior [$\chi = C/(T + \Theta)$], since both forms imply a decreasing susceptibility with increasing temperature, in contrast with the present observations. Neither is the observed continuous increase of the paramagnetic scattering with temperature expected in a Curie model. Nevertheless we will assume a Curie behavior in the following and we will discuss later on the anomalous temperature dependence of the susceptibility and the paramagnetic scattering.

At each temperature, the magnitude of $cS(S+1)$ can be deduced from the susceptibility measurement, using Eq. (5.2). Since at a given temperature the susceptibility is proportional to the Mn concentration [neglecting the small departure from the linear law observed for sample (a)] we can conclude that, at each temperature, the spin value is independent of c. Polarized neutron scattering experiments (Sec. IV C) on sample (a) demonstrated that the chemical incoherent scattering is equal to its maximal value in the liquid state. We shall assume that this is also true for the two other studied samples (b) ($\sigma_c = 0.46$ b) and (d) ($\sigma_c = 0.372$ b). Then the paramagnetic scattering can be deduced from the differential scattering cross section measured with unpolarized neutrons by using Eq. (4.1), with σ_i equal to 0.054, 0.043, and 0.039 b for samples (a), (b), and (d), respectively, and taking into account the temperature dependence of the density fluctuation term which remains in any case a small contribution. The $cS(S+1)$ values can then be deduced from the paramagnetic scattering, using Eq. (5.3) and compared to the $cS(S+1)$ values deduced from the susceptibility measurements, the only adjustable parameter of the comparison being $F^2(Q)$. The comparison is shown in Fig. 9 as a function of temperature for samples (a) $Al_{72.1}Pd_{20.7}Mn_{7.2}$, (b) $Al_{77}Pd_{18}Mn_5$, and (d) $Al_{76.5}Pd_{20}Mn_{3.5}$, using the 7C2 data at $Q = 0.7$ Å^{-1}. For each sample good agreement between both sets of $cS(S+1)$ data is obtained at all temperature in the liquid state with $F^2(Q = 0.7$ Å$^{-1})$ equal to 0.65, 0.76, and 0.83, respectively, for samples (a), (b), and (d). In Fig. 9 only the statistical errors are represented. Taking into account all the sources of error (see Secs. IV A and IV B) the error bar on $F^2(Q)$ is ± 0.12. For larger Q, at the highest temperature, the coherent nuclear scattering contributes to the measured differential scattering cross section because of the low Q resolution of the 7C2 spectrometer. For sample (a) the same analysis can be performed at smaller Q values, for $0.2 \leqslant Q \leqslant 0.7$ Å^{-1}, using the D4B data. The obtained $F^2(Q)$ value clearly decreases with increasing Q: $F^2(Q) = 0.92$ at $Q = 0.2$ AA^{-1}, to be compared to 0.77 at $Q = 0.7$ Å^{-1}. (This latter value differs from that found in Fig. 9 for the 7C2 data, which may be ascribed either to uncertainties in the signal treatment or to a slight sample composition difference.)

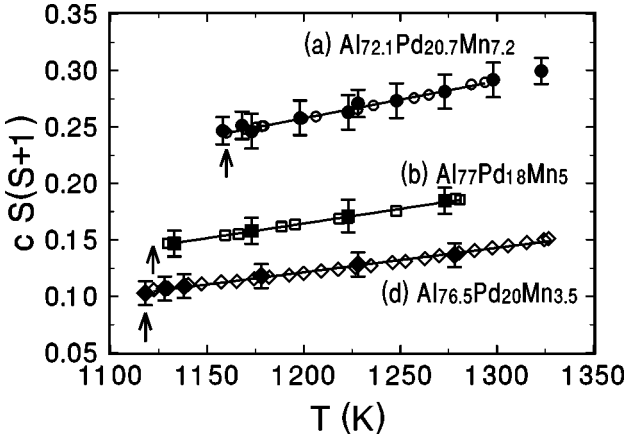

FIG. 9. Temperature dependence of $cS(S+1)$ in liquid Al-Pd-Mn alloys [samples (a), (b), and (d)]. The values deduced from the susceptibility data (presented in Fig. 6), using a Curie model, are shown by open symbols. (The solid lines are guides to the eye.) The error bars are smaller than the size of the symbols. The $cS(S+1)$ values deduced from the differential paramagnetic scattering cross section, at a fixed Q value (equal to 0.7 Å^{-1}), are shown by full symbols. For each sample, the squared magnetic form factor has been adjusted so that the both sets of data coincide: $F^2(Q=0.07\ \text{Å}^{-1})=0.65$ in sample (a), 0.76 in sample (b), and 0.83 in sample (d).

In conclusion the good agreement found between susceptibility and paramagnetic scattering data within a Curie model shows that both the temperature dependence of the susceptibility and that of the paramagnetic scattering in the liquid state of Al-Pd-Mn alloys can be ascribed to a continuous increase of $cS(S+1)$ when the temperature increases. Several features can be pointed out. (i) At a given temperature, the spin value is independent of c and the $cS(S+1)$ value is much smaller than the one obtained assuming that all the Mn atoms have a spin $S=5/2$. (ii) In the temperature range [1180–1280 K], where the comparison between susceptibility and paramagnetic scattering data could be performed, the increase of $S(S+1)$ with temperature is approximately linear: $S(S+1)$ is equal to 3.2 ± 0.2 at 1180 K and to 3.8 ± 0.2 at 1280 K. However, from the paramagnetic neutron scattering data on sample (a) (Fig. 5), it seems that the slope of this variation decreases at higher temperature: $S(S+1)$ is equal to 5.6 ± 0.4 at 1923 K. (iii) In several metallic liquid alloys containing $3d$ transition-metal impurities, departures from a simple Curie law were observed and described by writing $\chi=C/(T+\Theta)$, where Θ is a pseudo-Curie-Weiss temperature empirically introduced to account for Kondo effects.[44] Good agreement between neutron and susceptibility data could still be obtained in the temperature range [1180–1280 K] with $\Theta\sim300$ K but the small $F^2(Q)$ values obtained seem unreasonable. Thus in the following we will consider only a Curie law. (iv) We did not consider above the possible contribution to the Pauli susceptibility of Mn d states at the Fermi level. Such a contribution is expected to increase linearly with the Mn content and therefore cannot be separated from the Curie contribution. In a virtual bound state picture,[45] the d density of states at E_F is zero if the spin is equal to its maximum value 5/2, but this is no longer true if the spin value is reduced. Hence the $cS(S+1)$ values found above must be considered as the largest possible values in a Curie model.

The agreement between the spin values deduced from susceptibility and paramagnetic scattering data was obtained by introducing strikingly small values of the magnetic form factor. For comparison, for a Mn^{2+} free ion, $F^2(Q=0.7\ \text{Å}^{-1})=0.93$ and $F^2(Q=0.2\ \text{Å}^{-1})\simeq1$.[42] However, these values are compatible with the Q dependence of the paramagnetic scattering measured with polarized neutrons which, despite the experimental uncertainties, clearly differs from that of the Mn^{2+} magnetic form factor: see Fig. 8(a) where the right vertical axis proposes a normalization of the data to 1 at small Q. These observations raise doubts about our previous assumption of a single-ion behavior in Al-Pd-Mn liquids at 1170 K. One must consider either magnetic correlations leading to a Q-dependent static susceptibility, an anomalous magnetic form factor, or both effects. The continuous decrease of $F^2(Q=0.7\ \text{Å}^{-1})$ when the Mn concentration increases, deduced from the comparison between neutron and susceptibility data, would rather suggest the progressive establishment of magnetic correlations. Indeed the $F^2(Q=0.7\ \text{Å}^{-1})$ value for sample (d) is compatible with that for a free Mn^{2+} ion. In the presence of correlations, Eq. (5.3) is no longer valid and Eq. (5.1) should be used instead. Then the scaling factor between neutron and susceptibility data is no longer $F^2(Q)$ but rather $F^2(Q)\chi(Q)/\chi(Q=0)$.[43] It may seem surprising to observe magnetic correlations in liquid alloys at 1170 K. We also investigated with the same experimental setup a solid $Cu_{90}Mn_{10}$ alloy as a reference system (Ref. 39). At 1180 K in the solid state, similar deviations from the single-ion magnetic form factor were observed, which probably result from the presence of strong competing magnetic interactions in this alloy which incidentally gives rise to a spin glass transition at low temperature.

B. Local order in the solid and liquid states

The great similarity found between the structure factor of the liquid Al-Pd-Mn alloys and the diffraction spectrum in the solid quasicrystalline phase led us to assume the presence of a strong local icosahedral order in the liquids. In order to ascertain this hypothesis, we try in this section to analyze more quantitatively the liquid structure factor. Molecular dynamics is certainly the most powerful tool for determining liquid structures provided that the interaction potentials are known. It has been applied to a closely related liquid alloy $Al_{80}Mn_{20}$ in Ref. 16. An analysis of the coordination polyhedra does show the presence of local icosahedral order but without distinguishing between Al and Mn atoms. Here we will use simpler methods and show that the hypothesis of the presence of a strong icosahedral local order can at least be tested from theoretical considerations and from simulations of the measured structure factors at large Q.

First we compare the measured structure factors in the solid and in the liquid with the predictions of Sachdev and Nelson (Ref. 2) who described the structure factor of metallic glasses or supercooled liquids within a Landau theory, starting from an ideal icosahedral crystal imbedded in the surface of a four-dimensional (4D) sphere. These authors established that the existence of short-range icosahedral order in 3D pro-

duces broadened peaks of the structure factor at characteristic positions Q_A, Q_B, and Q_C linked by $Q_B/Q_A=1.707$ and $Q_C/Q_A=2.04$. In the diffraction spectrum of the icosahedral phase, four intense Bragg peaks (Q_0, Q_1, Q_2, Q_3) [with indices respectively given by (2/3,0/0,1/2), (2/4,0/0,0/0), (4/6,0/0,0/0), and (4/6,0/0,2/4) in the indexing scheme proposed by Cahn *et al.*[46]] can be easily identified [Fig. 1(a)]. They obey the relations $Q_1=1.052Q_0$, $Q_2=1.701Q_0$, and $Q_3=2.00Q_0$, with $Q_0=2.9952\pi/a_{6D}$ where a_{6D} is the 6D parameter of the icosahedral phase. Then comparing the solid and liquid structure factors of the $Al_{72.1}Pd_{20.7}Mn_{7.2}$ alloy [Figs. 1(a) and 2], it is clear that the first peak of the liquid structure corresponds to Q_0 and Q_1, while the second peak and its shoulder are directly related to Q_2 and Q_3. Then, by identifying Q_0 to Q_A, Q_2 to Q_B, and Q_3 to Q_C, as proposed in Ref. 3, it appears that the Sachdev and Nelson analysis perfectly accounts for the liquid structure factor of $Al_{72.1}Pd_{20.7}Mn_{7.2}$ above the melting point. The very similar structure factors of $Al_{76.5}Pd_{20}Mn_{3.5}$ and $Al_{77}Pd_{18}Mn_5$ liquid alloys can be described in the same way, although the Bragg peaks corresponding to the Sachdev and Nelson maxima are less well defined in the solid alloys which consist mainly of the ξ' approximant phase.[47] The same conclusion was previously drawn from the analysis of the liquid structure factor of liquid $Al_{80}Mn_{20}$ alloy in Ref. 15. However, the analysis was less convincing than in the present case because no structure factor in the solid state was measured. The existence of a shoulder on the second peak of the structure factor was also found in a slightly different approach by Sadoc *et al.*[48] who computed the structure factor of dense random packings of hard spheres with fivefold local symmetry. Hence, it is likely that in Al-Pd-Mn liquids, the existence of a shoulder in the second peak of the structure factor just above the melting temperature is related to the packing of entities with local icosahedral order. In such a case, the progressive attenuation of this shoulder, when temperature increases in the liquid state (see Fig. 4), should result from a progressive destruction either of the packing (medium distance range), of the icosahedral local order, or both.

The above approach remains qualitative. In order to try more quantitative analyses of the liquid structure factor, we first examined hard sphere models. The simulation shown in Fig. 10 follows the Ashcroft and Langreth derivation of the Percus-Yevick equation for a binary mixture[49] and the ternary liquid is assumed to be a pseudobinary system constituted of mean ''Al-Pd'' atoms and Mn atoms. The hard cores (2.31 Å for ''Al-Pd'' and 2.26 Å for Mn) and the packing fraction (0.413) are chosen in order to fit the first peak of the structure factor. It is clear that a hard sphere model is unable to account for the positions and intensities of the oscillations of the structure factor at larger Q.

Although simulations of the measured structure factors in the whole Q range are a very complex task, an analysis of the structure factor at large Q is possible under several conditions and indeed brings very interesting information on the local order. The principle of the method, initially introduced to describe molecular solids.[51–53] is explained in the Appendix. Its application to liquid Al-Pd-Mn alloys implies that a cluster can be defined in the liquid and that the atoms within the cluster are more rigidly bound together than to other atoms in the system. Note that this method does not allow

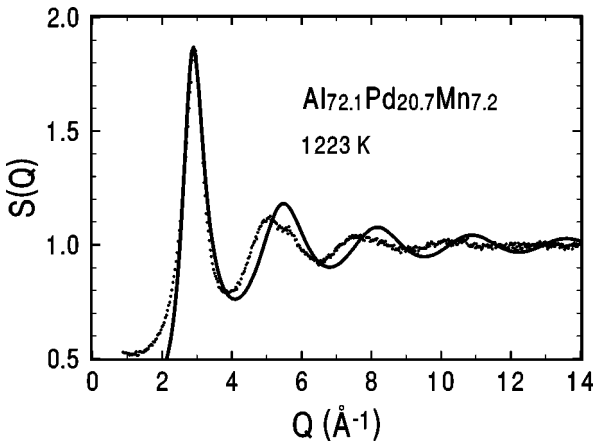

FIG. 10. Comparison of the measured structure factor at 1223 K (dots) in $Al_{72.1}Pd_{20.7}Mn_{7.2}$ with the results of a hard sphere simulation. The parameters of the simulation (see text) were chosen in order to fit the first peak.

one to determine the structure and the chemistry of the cluster but indicates whether a given cluster model is compatible with the data or not by comparing at large Q the calculated structure factor [using Eq. (A2)] to the measured one. In the Q range where the comparison is done ($4.5 \leqslant Q \leqslant 16$ Å^{-1}), the paramagnetic contribution is zero (Sec. IV C) and the experimental structure factor $S_{exp}(Q)$ can be compared to the theoretical one.

Because of the similarity between local order in the icosahedral solid and in the liquid, the choice of the cluster was guided by the structural description of several Al-Mn (Ref. 50) and Al-Pd-Mn (Ref. 19) approximant phases. A cluster of 1 Mn atom surrounded by 12 Al atoms on the vertices of an icosahedron is a major constituent of these phases. The $Al_{12}Mn$ intermetallic compound can be described as a body-centered cubic packing of these icosahedral clusters. Even complex structures, such as μ-Al_4Mn, can be described in terms of these icosahedra. In this latter case the icosahedra are linked in different ways, or interpenetrate, resulting in a substitution by Mn atoms of 1 or 2 Al on the icosahedral shell. In the ξ' Al-Pd-Mn approximant there are two Mn sites: one is surrounded by 12 Al at the vertices of an icosahedron and the other one is surrounded by a disordered first shell of approximately 11 Al and a second shell defined as a perfect Pd icosahedron (Ref. 19). Note that similar clusters have also been identified in the icosahedral Al-Pd-Mn quasicrystal (Ref. 9).

We first tried to simulate the measured structure factor of sample (a) ($Al_{72.1}Pd_{20.7}Mn_{7.2}$) at 1223 K by assuming the presence of $Al_{12}Mn$ icosahedra. Taking the alloy composition into account and assuming that all the Al atoms form icosahedra, only 78% of all the atoms (and 83% of the Mn atoms) can be included in such clusters. The parameters are the mean distance from the center to a vertex of the icosahedron ($\langle r_0 \rangle$) and the mean thermal variation of this distance ($\langle \delta r_0^2 \rangle$). The three other distances within the icosahedron are $\langle r_1 \rangle = 1.0515 \langle r_0 \rangle$, $\langle r_2 \rangle = 1.7013 \langle r_0 \rangle$, $\langle r_3 \rangle = 2 \langle r_0 \rangle$ [see the inset of Fig. 11(b)]. We assumed that the mean thermal variations of these distances $\langle \delta r_i^2 \rangle$ are equal to $\langle \delta r_0^2 \rangle (\langle r_i \rangle / \langle r_0 \rangle)^2$.[54] The structure factor calculated with $\langle r_0 \rangle = 2.44$ Å and $\langle \delta r_0^2 \rangle = 0.046$ Å^2 is drawn in Fig. 11(a). It

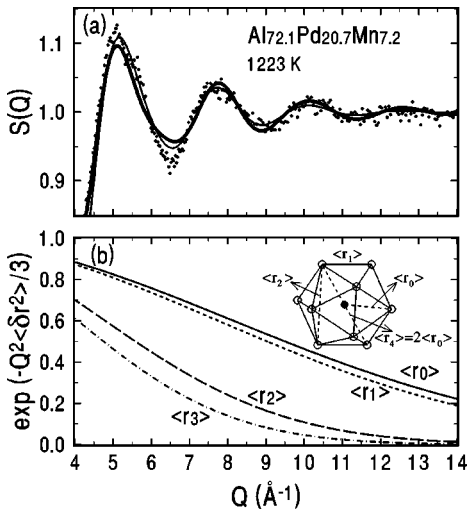

FIG. 11. (a): Comparison for $Q \geq 4.5$ Å^{-1} of the measured structure factor at 1223 K in $Al_{72.1}Pd_{20.7}Mn_{7.2}$ (dots) with the calculated structure factor assuming $Al_{12}Mn$ icosahedra (thick solid line) and $(Al_{0.777}Pd_{0.223})_{12}Mn$ icosahedra (thin solid line): see text. (b) Q dependence of the Debye-Waller factors for the four pair distances within the $Al_{12}Mn$ icosahedron [$\langle r_0 \rangle = 2.44$ Å, $\langle \delta r_0^2 \rangle = 0.046$ Å^2 and $\langle \delta r_i^2 \rangle = \langle \delta r_0^2 \rangle (\langle r_i \rangle / \langle r_0 \rangle)^2$].

well describes the measured data for $Q \geq 7$ Å^{-1}. The found agreement is very sensitive to the $\langle r_0 \rangle$ value which is therefore accurately determined (± 0.03 Å). It is interesting to note that the Al-Mn distance within the icosahedron deduced from the simulation (2.44 Å) is very close to the short Al-Mn distances observed in the ξ' structure (2.49 Å) in Ref. 19. Simulations assuming a lower proportion of icosahedra (involving less than 70% of the atoms) are unable to account for the amplitude of the oscillations of the structure factor at large Q. Although the above analysis can fairly well account for the measured data at large Q, a weak point of the simulation of the structure factors by Al_{12} Mn icosahedra is to exclude Pd atoms. Thus we also tried to simulate the structure factor of sample (a) by assuming that all the Mn atoms are at the center of $(Al_{0.777}Pd_{0.223})_{12}$ icosahedra. The relative proportion of Al and Pd atoms in the icosahedron is chosen to match the alloy composition. In this hypothesis 94% of the atoms belong to clusters. A good simulation of the data is obtained with the same $\langle r_0 \rangle$ value and a slightly larger $\langle \delta r_0^2 \rangle$ value (0.073 Å^2) than for the $Al_{12}Mn$ icosahedron. Indeed the two simulations are nearly indiscernible in the Q-range [7–16 Å^{-1}] [see Fig. 11(a)]. In the Q range [4.5–7 Å^{-1}] the agreement is slightly better for the Al-Pd icosahedron. However, in this Q range, intercluster terms may also contribute to the measured structure factor and make it difficult to discriminate between different hypothesis for the intracluster contribution. However, one should emphasize that such a Al-Pd cluster is not encountered in approximant phases. A better way to include the Pd atoms is perhaps to assume that all the Mn atoms are embedded in Al_{12} Mn icosahedra and that some of these icosahedra are surrounded by a second icosahedral shell made of Pd atoms, as observed in the ξ' Al-Pd-Mn approximant. We checked that adding a Pd icosahedron around the Al_{12} Mn icosahedron does not modify the general trends of the calculated structure factor. We did not try a simulation of the data because of the too large number of adjustable parameters in such a model. For samples (b) and (d), with lower Mn content, good descriptions of the experimental structure factors measured can be obtained assuming that some of the Al_{12} icosahedra are centered on Al or Pd atoms. (Considering only icosahedra centered on Mn atoms leads to a too small proportion of atoms in clusters.) Al icosahedra centered on a Pd atom are indeed found in the orthorhombic Al_3 Pd phase (Ref. 24).

In order to determine in which Q range the comparison of the calculated and measured structure factors is really meaningful, we have calculated the Debye-Waller factors at 1223 K for the four pair distances in the $Al_{12}Mn$ icosahedron [see Fig. 11(b)]. For $Q \geq 8$ Å^{-1}, Debye-Waller factors related to the two shortest distances $\langle r_0 \rangle$ and $\langle r_1 \rangle$ appear to be the leading contribution. Then the good agreement found between the simulation and the data for $Q \geq 8$ Å^{-1} demonstrates that other short distances in the system (between clusters) do not play an important role. This means that the Debye-Waller factors corresponding to intercluster distances are more rapidly damped when Q increases than those corresponding to intracluster distances and justifies, *a posteriori*, the assumption of clusters where the atoms are rigidly bound together. In addition, the $\langle \delta r_0^2 \rangle$ value deduced from the simulations at 1223 K are roughly compatible with the averaged mean thermal variation of atomic positions in the ξ' approximant phase at 300 K.

Because of the similarity found between the oscillations of the structure factor at large Q in the solid and liquid states, it seems quite natural to assume that the short-range order in the liquid is based on the icosahedral clusters found in the solid. Nevertheless we have tried simulations based on other kinds of densely packed clusters of 13 atoms (with the coordination polyhedra of the fcc or hcp lattice). At low temperature such simulations clearly differ from those obtained assuming icosahedral clusters, as previously shown in Ref. 48. At 1170 K these differences are strongly reduced at large Q, because of the Debye-Waller effect. However, the hypothesis of an icosahedral cluster provides the best simulation in the medium Q range ($4.5 \leq Q \leq 7$ Å^{-1}).

In summary the measured structure factors in Al-Pd-Mn alloys are compatible with the presence of a strong local icosahedral order in the liquid state, reminiscent of that in the solid. The best results are obtained when a large proportion of the atoms belong to icosahedral clusters. The rigid binding of atoms within the clusters is suggested by two features: (i) the Debye-Waller factor in the liquid is related to that in an approximant phase, (ii) the pair distances in the liquid are very close to those in solids.

VI. DISCUSSION

The results presented above imply that liquid Al-Pd-Mn alloys in equilibrium with quasicrystalline or approximant phases exhibit remarkable magnetic and structural properties. First, magnetic localized moments on Mn atoms exist in the liquid state. Although the Q dependence of the paramagnetic scattering suggests the presence of Mn-Mn correlations, a dilute alloy picture seems to be valid as a first approximation because, at a given temperature, the susceptibility increases linearly with the Mn concentration and tends towards the susceptibility of the Al-Pd matrix when the Mn concentra-

tion tends to zero. Secondly, as shown in Sec. V A, at any fixed temperature, the same spin value S, independent of the Mn content, is drawn in a simple Curie model from the susceptibility and the paramagnetic scattering data, although their temperature dependence is in obvious contradiction with the Curie model. This shows that the continuous increase of the susceptibility and of the paramagnetic scattering with temperature in the liquid state have the same origin and must be ascribed to a continuous increase of the $cS(S+1)$ value with temperature. Schematically two kinds of hypothesis might be considered. First, if all the Mn atoms are magnetic at T_L, as implicitly assumed up to now, the only possible explanation is an increase of the spin value with temperature in the liquid state. Within this hypothesis, the spin value at 1180 K (1.36 ± 0.05) is indeed much smaller than its maximal possible value (5/2) and reaches 1.91 ± 0.09 at 1923 K. Secondly, if only a fraction of the Mn atoms are magnetic at the melting temperature T_L, one can consider an increase in the proportion of magnetic atoms when the temperature increases, in addition to the possible increase of their spin value. Let c^* be the concentration of magnetic Mn. One consequence of the linear increase of χ with the total Mn concentration is that the ratio c^*/c must be independent of c. The comparison between neutron and susceptibility data performed in Sec. V A remains unchanged, as long as we assume that all the magnetic Mn atoms contribute equally to the magnetic scattering, and allows one to determine $c^*S(S+1)$. The minimum value of c^*/c, obtained by assuming $S=5/2$, is of the order of 0.35 at 1180 K and 0.65 at 1923 K. (If the spin value is smaller, then c^*/c increases).

Before reviewing the implications of both these hypotheses let us first make a few comments on magnetism in the liquid and solid states of Al-Pd-Mn alloys. First it seems that the Pd atoms do not play an important role. Indeed the magnetic susceptibilities measured in Al-Pd-Mn alloys are very close to values found in dilute liquid Al_{100-c} Mn_c alloys with $c \leqslant 5$,[55] where a linear dependence of χ upon the Mn concentration has also been observed. Moreover in liquid $Al_{100-c}Mn_c$, the susceptibility also increases with temperature in the liquid state. It is striking to notice that among the many studied metallic liquid hosts containing Mn atoms (Ref. 44), this strange behavior is observed only in $Al_{100-c}Mn_c$. The presence of paramagnetic scattering in the liquid $Al_{80}Mn_{20}$ alloy above its melting point was suggested in Ref. 15 but no study of its temperature dependence was performed. Secondly, the solid Al-Pd-Mn phases with similar compositions are found either to be nonmagnetic or to exhibit only small Curie terms. Here the term ''nonmagnetic'' means that no Curie behavior is detected and that the measured susceptibility (sum of the conduction electron and Larmor contributions) is temperature independent (apart from a possible T^2 term due to the presence of a pseudogap at the Fermi level, see Sec. IV B). We measured a single crystal of the approximant ξ' phase and found that it is nonmagnetic. Curie terms have been reported in quasicrystalline Al-Pd-Mn phases.[36,56] The Curie constant C increases very rapidly when the Mn content increases but even in the more concentrated alloys, C remains small and only a few percent of all Mn atoms bear a moment. Moreover the observation of a Mn nuclear magnetic resonance signal[57] in quasicrystalline Al-Pd-Mn alloys gives more evidence that most of the Mn atoms bear no localized magnetic moment, because the Mn nuclei located on the site of a magnetic moment cannot be detected. Therefore, magnetism in the solid Al-Pd-Mn quasicrystals concerns only a small fraction of the Mn sites, whereas in the liquid all, or at least a large proportion of the Mn sites, are concerned. The jump in the susceptibility at the melting point is thus the direct consequence of the formation of moments in the liquid. A similar temperature dependence of the susceptibility has previously been observed when melting $Al_{65}Cu_{20}Co_{15}$ and $Al_{70}Ni_{15}Co_{15}$ decagonal phases.[58] In the absence of data on other samples with different Co compositions or of neutron scattering data, an abrupt change of the Pauli susceptibility upon melting could be proposed. However, in view of the similarity between these data and ours, the hypothesis of magnetic moments on Co atoms in the liquid should also be considered.

Then one must wonder why liquids are magnetic and why this magnetism disappears in the solid state. In the solid, the pseudogap and $sp-d$ hybridization[21] could play an important role in preventing the formation of a localized moment. However, considerations of Mn-Mn nearest distances in the solid are also important. From the analysis of the Mn-Mn interaction potentials, it seems that the appearance of a magnetic moment is quite unfavorable for several Mn-Mn distances (Ref. 22) which are the preferred ones in most solid phases.[59] Thus the effect of melting would schematically be twofold. First the pseudogap is attenuated in the liquid, although probably not completely erased. Secondly several Mn-Mn distances, for which the formation of a magnetic moment is favorable, can occur. At this stage it would be worth knowing whether dilute Mn atoms in a fcc Al matrix are magnetic or not. Although contradictory answers are found in the literature, it seems that such Mn atoms are magnetic, this magnetism being possibly attenuated by a Kondo effect (see Ref. 60, and references therein). In the liquid, *ab initio* calculations of several $Al_{100-c}Mn_c$ alloys ($14 \leqslant c \leqslant 40$) have predicted the occurrence of magnetic moments ascribed to topological disorder in the liquid.[61] The moment magnitude $3.3\mu_B$ (corresponding to a spin value $S=1.65$, assuming $g=2$) is compatible with the values that we found in Al-Pd-Mn alloys. However, because of the extreme sensitivity of magnetism to the local structure, this agreement must be considered as only a good hint. A quantitative comparison of these theoretical predictions with our results is not really meaningful because it is unclear whether the liquid structure used to calculate the electronic properties in Ref. 61 can describe the Al-Pd-Mn liquid alloys studied here which have a much smaller Mn content. However, it is interesting to note that the moment found in the simulations decreases with the Mn content and that Mn-Mn interactions are detected in Al-Mn liquids. This observation could be related to the anomalous Q dependence of the paramagnetic scattering in $Al_{72.1}$ $Pd_{20.7}$ $Mn_{7.2}$ at 1170 K.

Let us now discuss the possible origin of the continuous increase of magnetism with the temperature, in relation to the evolution of the liquid structure. One must first discuss the consequences of thermal expansion which indeed could lead to an increase of the spin value. Results can be found in the literature for the case of Fe embedded in an Al cluster.[62] The magnetic moment on Fe, absent for Fe-Al distances

shorter than the critical threshold, appears at the threshold and then continues to increase with the Fe-Al distance. In this latter regime, a relative distance change of 0.4% (which could be expected in liquid Al-Pd-Mn alloys when temperature increases from 1180 to 1280 K, using the thermal expansion of Al), would cause a relative increase of the spin value of 3%. As the observed relative increase of the spin value is 11%, it seems unlikely that it would be entirely caused by a thermal expansion effect and modifications of the liquid structure should be envisaged. Calculations of the magnetic moment of a Mn atom in an Al matrix as a function of the Al-Mn distance would, of course, be necessary to better estimate the consequences of thermal expansion. In addition, it seems that the density change on melting is not sufficient to trigger the appearance of a magnetic moment in the liquid (its amplitude is probably too small and moreover such an effect would imply that the critical Al-Mn distance for the formation of a moment is exactly met on melting which seems quite unlikely). Dilatation would be the only possible origin of a continuous increase of S, if all the Mn were magnetic at T_L and if the liquid structure was temperature independent. However, in the case of nonhomogeneous magnetism, another possibility is that the fraction of magnetic Mn atoms (i.e., c^*/c) increases with temperature because of modifications of the liquid structure. In this framework, the simplest hypothesis is to assume that a Mn atom with a local environment close to that in the solid remains nonmagnetic in the liquid just above T_L. This could be the case of Mn atoms embedded in an Al icosahedron, while Mn atoms in another environment would be magnetic. In this framework one must in addition assume that clusters are progressively destroyed with increasing temperature. However, this hypothesis requires that at least 35% of the Mn atoms are magnetic (with $S=5/2$) at T_L and is not in good agreement with the results of the simulations of the structure factor at large Q which rather suggest that most of the Mn atoms are embedded in Al_{12} icosahedra. Another hypothesis is to consider dynamical fluctuations of the clusters around their mean equilibrium shape. In this latter case a given Mn atom within an icosahedral shell could change from a magnetic to a nonmagnetic state as a function of time. The only requirement would be that a magnetic Mn must survive for a time long enough to be observed by neutron scattering. Thus it is difficult to conclude as both short- and medium-range orders are important for magnetism. Accurate simulations on realistic liquid models would be one way to validate this hypothesis on the existence of magnetic and nonmagnetic Mn in liquid Al-Pd-Mn alloys.

In conclusion we think that a strong local icosahedral order exists in liquid Al-Pd-Mn alloys and is probably determinant to understand their magnetic properties. The fact that clusters existing in crystalline approximant phases subsist in the liquid state suggests a high stability of these clusters as indeed found in calculations of isolated Al_{12} Mn clusters.[63] Modifications in the liquid structure as a function of temperature, such as changing Mn environments, give the most likely explanation for the temperature-dependent magnetic properties of liquid Al-Pd-Mn alloys.

ACKNOWLEDGMENTS

We thank J. P. Ambroise for designing the experimental setup for neutron scattering on the 7C2 spectrometer, P. Palleau for reconstructing and improving the D4B high-temperature furnace and for his faithful assistance during the neutron experiments at D4B, Dr. O. Schärpf and Dr. K. Andersen for their help during the experiments on D7. This work has benefited from many fruitful discussions with Dr. J. Blétry on local order, and with Dr. G. Trambly de Laissardière and Dr. I. A. Campbell on the origin of magnetism in liquid and solid Al-Pd-Mn alloys.

APPENDIX: NEUTRON SCATTERING BY A MOLECULAR SYSTEM

We recall here the main results for neutron scattering by a system of N particles constituted of N_m identical molecules, each molecule containing $N_{\rm at}$ atoms (Refs. 51–53). Let us assume that one can split the atomic position fluctuations around their mean values into translational motion of the molecular center of mass around its mean value and intramolecular motions. Then one can introduce $\exp(-2W)$, the Debye-Waller factor relative to the motion of the center of mass of the molecule, and $\exp(-2W_{kl})$, the Debye-Waller factor corresponding to the thermal changes ($\langle \delta r_{kl} \rangle$) of the distance r_{kl} between atoms k and l belonging to the same molecule, due to the internal motions of the molecule. In the harmonic approximation $2W_{kl}=\frac{1}{3}Q^2\langle \delta r_{kl}^2 \rangle$. (In order to compare this expression with the usual Debye-Waller factors in atomic systems one should consider that for first neighbors $\langle \delta r_{kl}^2 \rangle$ is equal to $\langle u_k^2 \rangle + \langle u_l^2 \rangle$, where $\langle u_k^2 \rangle$ and $\langle u_l^2 \rangle$ are the mean thermal fluctuation of the kth and lth atom positions, respectively.) For large enough Q, $\exp(-2W)$ is vanishing, while $\exp(-2W_{kl})$ remains finite because the atoms within the molecule are rigidly bound together while the molecules are only weakly coupled. Therefore the differential scattering cross section per atom $d\sigma/d\Omega$ reduces at large Q to the intramolecular contribution which is equal to $N_m\langle F^2(Q)\rangle/N$, where $\langle F(Q)\rangle$ is the molecular form factor and the brackets stand for the thermodynamic average. For identical quasi-spherical molecules, or molecules with random orientation, $\langle F^2(Q)\rangle$ is given by (Ref. 53)

$$\langle F^2(Q)\rangle = \sum_{k,l=1(k\neq l)}^{N_{\rm at}} \overline{b_k}\,\overline{b_l}\frac{\sin(Q\langle r_{kl}\rangle)}{Q\langle r_{kl}\rangle}\exp(-2W_{kl}) + \sum_{k=1}^{N_{\rm at}} \overline{b_k}^2 + \sum_{k=1}^{N_{\rm at}} \frac{\sigma_{\rm inc}^k}{4\pi}, \tag{A1}$$

where $\langle r_{kl}\rangle$ is the average value of the distance between atoms k and l within the molecule, $\overline{b_k}$ is the mean scattering length, and $\sigma_{\rm inc}^k$ the incoherent cross section of atom k. Hence, at large Q, the structure factor $S(Q)=[4\pi(d\sigma/d\Omega)-\sigma_i]/(4\pi\langle b^2\rangle)$ (where $\langle b^2\rangle=\Sigma_j c_j \overline{b_j}^2$ and $\sigma_i=\Sigma_j c_j \sigma_{\rm inc}^j$, c_j is the concentration of the jth element in the system) is given by

$$S(Q)-1=\frac{1}{N_{\rm at}\langle b^2\rangle}\sum_{k,l=1(k\neq l)}^{N_{\rm at}} \overline{b_k}\,\overline{b_l}\frac{\sin(Q\langle r_{kl}\rangle)}{Q\langle r_{kl}\rangle} \times \exp(-2W_{kl}). \tag{A2}$$

This formalism has been successfully applied to molecular systems in Refs. 52,53. Here we used it in Sec. V B to de-

scribe the high Q-range part of the structure factor of liquid Al-Pd-Mn alloys, assuming the existence of well-defined clusters in the liquid. One requirement is that clusters have a lifetime τ_c compatible with thermal neutron scattering (i.e., $\tau_c \geqslant 10^{-10}$ s). Another requirement is that atoms within the clusters are much more rigidly bound together than to atoms belonging to other clusters. Note that in the previous formalism the chemical composition of the molecule and that of the system are identical and that all the atoms belong to molecules ($N = N_m N_{at}$). In the case of Al-Pd-Mn alloys, this requirement is not necessarily fulfilled by the clusters, and a multiplicative factor $N_m N_{at}/N$ must be introduced in Eq. (A2).

[1] D. Shechtman, I. Blech, D. Gratias, and J. W. Cahn, Phys. Rev. Lett. **53**, 1951 (1984).

[2] S. Sachdev and D. R. Nelson, Phys. Rev. Lett. **53**, 1947 (1984).

[3] S. Sachdev and D. R. Nelson, Phys. Rev. B **32**, 4592 (1985).

[4] F. C. Frank, Proc. R. Soc. London, Ser. A **215**, 43 (1952).

[5] P. J. Steinhardt, D. R. Nelson, and M. Ronchetti, Phys. Rev. B **28**, 784 (1983).

[6] D. Shechtman and I. Blech, Metall. Trans. A **16**, 332 (1985); P. W. Stephens and A. I. Goldman, Phys. Rev. Lett. **56**, 1168 (1986).

[7] P. J. Steinhardt and S. Ostlund, *The Physics of Quasicrystals* (World Scientific, Singapore, 1987).

[8] M. Cornier-Quiquandon, A. Quivy, S. Lefebvre, E. Elkaim, G. Heger, A. Katz, and D. Gratias, Phys. Rev. B **44**, 2071 (1991).

[9] M. Boudard, M. de Boissieu, C. Janot, G. Heger, C. Beeli, H. U. Nissen, P. Vincent, R. Ibberson, M. Audier, and J. M. Dubois, J. Phys.: Condens. Matter **4**, 10 149 (1992).

[10] D. Mayou, C. Berger, F. Cyrot-Lackmann, T. Klein, and P. Lanco, Phys. Rev. Lett. **70**, 3915 (1993); B. D. Biggs, S. J. Poon, and N. R. Munirathnam, *ibid.* **65**, 2700 (1990).

[11] A. L. Mackay, Acta Crystallogr. **15**, 916 (1962); G. Bergman, J. L. T. Waugh, and L. Pauling, *ibid.* **10**, 254 (1957).

[12] V. Elser and C. L. Henley, Phys. Rev. Lett. **55**, 2883 (1985); P. Guyot and M. Audier, Philos. Mag. B **52**, L15 (1985); C. L. Henley and V. Elser, *ibid.* **53**, L59 (1986); M. Duneau and C. Oguey, J. Phys. (Paris) **50**, 135 (1989); C. Janot, *Quasicrystals, a Primer* (Clarendon, Oxford, 1992).

[13] C. Janot and M. De Boissieu, Phys. Rev. Lett. **72**, 1674 (1994).

[14] T. Fujiwara, S. Yamamoto, and G. Trambly de Laissardière, Phys. Rev. Lett. **71**, 4166 (1993); G. Trambly de Laissardière and D. Mayou, Phys. Rev. B **55**, 2890 (1997).

[15] M. Maret, A. Pasturel, C. Senillou, J. M. Dubois, and P. Chieux, J. Phys. (France) **50**, 295 (1989); M. Maret, P. Chieux, J. M. Dubois, and A. Pasturel, J. Phys.: Condens. Matter **3**, 2801 (1991); M. Maret, J. M. Dubois, and P. Chieux, J. Non-Cryst. Solids **156-158**, 918 (1993).

[16] M. Maret, F. Lançon, and L. Billard, J. Phys. I **3**, 1873 (1993); L. Do Phuong, D. Nguyen Manh, and A. Pasturel, J. Phys.: Condens. Matter **6**, 2853 (1994).

[17] M. Audier, M. Durand-Charre, and M. de Boissieu, Philos. Mag. B **68**, 607 (1993).

[18] Y. Yokoyama, A. P. Tsai, A. Inoue, and T. Masumoto, Mater. Trans., JIM **22**, 1089 (1991); T. Gödecke and R. Lück, Z. Metallkd. **86**, 109 (1995).

[19] M. Boudard, H. Klein, M. de Boissieu, M. Audier, and H. Vincent, Philos. Mag. A **74**, 939 (1996); H. Klein, M. Boudard, M. de Boissieu, M. Audier, H. Vincent, L. Beraha, and M. Duneau, Philos. Mag. Lett. **75**, 197 (1996).

[20] F. Hippert, M. Audier, H. Klein, R. Bellissent, and D. Boursier, Phys. Rev. Lett. **76**, 54 (1996).

[21] G. Trambly de Laissardière, D. Mayou, and D. Nguyen Manh, Europhys. Lett. **21**, 25 (1993).

[22] G. Trambly de Laissardière and D. Mayou, in *Introduction to the Physics of Quasicrystals*, edited by J. B. Suck (Springer, Berlin, in press).

[23] W. Hume-Rothery and G. V. Raynor, *The Structure of Metals and Alloys* (Institute of Metals, London, 1954); J. Friedel and F. Denoyer, C. R. Acad. Sci., Ser. II: Mec. Phys., Chim., Sci. Terre Univers **305**, 171 (1987); S. J. Poon, Adv. Phys. **41**, 303 (1992).

[24] Y. Matsuo and K. Hiraga, Philos. Mag. Lett. **70**, 155 (1994).

[25] J. Blétry, P. Tavernière, C. Senillou, P. Desré, M. Maret, and P. Chieux, Rev. Phys. Appl. **19**, 725 (1984).

[26] V. F. Sears, Atomic Energy of Canada Limited Report No. AECL-8490, Chalk River, 1984 (unpublished).

[27] H. H. Paalman and C. J. Pings, J. Appl. Phys. **33**, 2635 (1962).

[28] G. Placzek, Phys. Rev. **86**, 377 (1952).

[29] J. L. Yarnell, M. J. Katz, R. G. Wenzel, and S. H. Koenig, Phys. Rev. A **7**, 2130 (1973).

[30] I. A. Blech and B. L. Averbach, Phys. Rev. **137**, A1113 (1965).

[31] A. B. Bhatia and D. E. Thornton, Phys. Rev. B **2**, 3004 (1970).

[32] N. H. March, *Liquid Metals, Concepts and Theory* (Cambridge University Press, Cambridge, 1990).

[33] V. I. Stremousov and V. V. Tekuchev, Russ. J. Phys. Chem. **51**, 206 (1977).

[34] P. Ascarelli, Phys. Rev. **173**, 271 (1968).

[35] S. Matsuo, T. Ishimasa, H. Nakano, and Y. Fukano, J. Phys.: Condens. Matter **1**, 6893 (1989).

[36] K. Saito, S. Matsuo, H. Nakano, T. Ishimasa, and M. Mori, J. Phys. Soc. Jpn. **63**, 1940 (1994); A. Kobayashi, S. Matsuo, T. Ishimasa, and H. Nakano, J. Phys.: Condens. Matter **9**, 3205 (1997).

[37] O. Schärpf and H. Capellman, Phys. Status Solidi A **135**, 359 (1993).

[38] The isotopic incoherent scattering of Al and Mn is equal to zero. For Pd both isotopic and spin disorder occur but the available data do not allow a separation of the two contributions. Therefore, by using the total incoherent scattering of Pd (0.093 b) we have maximized the isotopic incoherent scattering in the $Al_{72.1}\,Pd_{20.7}\,Mn_{7.2}$ alloy.

[39] A. P. Murani, J. Magn. Magn. Mater. **25**, 68 (1981).

[40] Assuming that the paramagnetic scattering is single-ion-like and that the spectral response is given by a Lorentzian with half width Γ, then Γ would be roughly of the order of 20–30 meV at 1170 K. This value can be compared with that for Mn ions in Cu in the dilute limit [$\Gamma = 9$ meV from an extrapolation at 1170 K of the room temperature value, assuming a Korringa law behavior (Ref. 39)].

[41] W. Marshall and R. D. Lowde, Rep. Prog. Phys. **31**, 705 (1968); S. W. Lovesey, *Theory of Neutron Scattering from Condensed Matter* (Clarendon, Oxford, 1984).

[42] R. E. Watson and A. J. Freeman, Acta Crystallogr. **14**, 27 (1961); P. J. Brown, *International Tables for Crystallography*, edited by A. J. C. Wilson (Kluwer Academic, Dordrecht, 1992), Vol. C.

[43] In the presence of magnetic correlations, the spectral width of the paramagnetic scattering is Q dependent. Then the Q dependence of the signal detected on the spectrometer D7 can slightly differ from that of the total paramagnetic scattering, because of the restricted energy integration range.

[44] J. J. Peters and C. P. Flynn, Phys. Rev. B **6**, 3343 (1972).

[45] P. W. Anderson, Phys. Rev. **124**, 41 (1961).

[46] J. W. Cahn, D. Schechtman, and D. Gratias, J. Mater. Res. **1**, 13 (1986).

[47] In a previous paper [H. Klein, L. Descôtes, M. Audier, R. Bellissent, and F. Hippert, J. Non-Cryst. Solids **205-207**, 6 (1996)] we had applied the same analysis to less accurate data and could not draw precise conclusions for the $Al_{76.5}Pd_{20}Mn_{3.5}$ alloy.

[48] J. F. Sadoc, J. Dixmier, and A. Guinier, J. Non-Cryst. Solids **12**, 46 (1973).

[49] N. W. Ashcroft and D. C. Langreth, Phys. Rev. **156**, 685 (1967).

[50] J. Adam and J. B. Rich, Acta Crystallogr. **7**, 813 (1954); M. Cooper and K. Robinson, *ibid.* **20**, 614 (1966); G. Kreiner and H. F. Franzen, J. Alloys Compd. **202**, L21 (1993); T. Schenk, H. Klein, M. Audier, V. Simonet, F. Hippert, J. Rodriguez-Carvajal, and R. Bellissent, Philos. Mag. Lett. **76**, 189 (1997).

[51] G. Dolling, B. M. Powell, and V. F. Sears, Mol. Phys. **6**, 37 (1979).

[52] P. Damay, F. Leclercq, and P. Chieux, Phys. Rev. B **41**, 9676 (1990).

[53] F. Leclercq, P. Damay, M. Foukani, P. Chieux, M. C. Bellissent-Funel, A. Rassat, and C. Fabre, Phys. Rev. B **48**, 2748 (1993).

[54] A linear law $\langle \delta r_i^2 \rangle = \langle \delta r_0^2 \rangle \langle r_i \rangle / \langle r_0 \rangle$, as proposed in Ref. 53, leads to a poorer agreement in the Q range [4.5–7 $Å^{-1}$], but in this Q range intercluster terms may also contribute to the measured structure factor and mask some features of the intracluster contribution.

[55] C. P. Flynn, D. A. Rigney, and J. A. Gardner, Philos. Mag. **15**, 1255 (1967).

[56] M. A. Chernikov, A. Bernasconi, C. Beeli, A. Schilling, and H. R. Ott, Phys. Rev. B **48**, 3058 (1993); Y. Hattori, K. Fukamichi, H. Chikama, H. Aruga-Katori, and T. Goto, J. Phys.: Condens. Matter **6**, 10 129 (1994); J. C. Lasjaunias, A. Sulpice, N. Keller, J. J. Préjean, and M. de Boissieu, Phys. Rev. B **52**, 886 (1995).

[57] T. Shinohora, A. P. Tsai, and T. Masumoto, J. Phys.: Condens. Matter **4**, 3043 (1992).

[58] R. Lück, and S. Kek, J. Non-Cryst. Solids **153-154**, 329 (1993).

[59] J. Zhou and A. E. Carlsson, Phys. Rev. Lett. **70**, 3748 (1993).

[60] S. L. Yang, H. B. Lan, K. L. Wang, L. F. Donà dalle Rose, and F. Toigo, Phys. Rev. B **44**, 10 508 (1991).

[61] A. M. Bratkovsky, A. V. Smirnov, D. Nguyen Manh, and A. Pasturel, Phys. Rev. B **52**, 3056 (1995); A. V. Smirnov and A. M. Bratkovsky, *ibid.* **53**, 8515 (1996).

[62] D. Guenzburger and D. E. Ellis, Phys. Rev. Lett. **67**, 3832 (1991).

[63] X. G. Gong and V. Kumar, Phys. Rev. B **50**, 17 701 (1994).